

Mook

Ira R. Schwartz

N71-20194

NASA CR-117180

RE-371

SCATTERING OF EPITHERMAL ARGON
BY (111) SILVER SURFACES:
A COMPARISON OF THEORY
AND EXPERIMENT

September 1969

CASE FILE
COPY

Grumman

RESEARCH DEPARTMENT



GRUMMAN AIRCRAFT ENGINEERING CORPORATION
BETHPAGE NEW YORK

SCATTERING OF EPITHERMAL ARGON BY (111) SILVER
SURFACES: A COMPARISON OF THEORY AND EXPERIMENT[†]

by

V. S. Calia

and

R. A. Oman

Fluid Mechanics Section

September 1969

[†]This work was sponsored by NASA Office of Advanced Research and Technology, Fluid Dynamics Branch, under Contract NASw-1461.

Approved by: *Charles E. Mack, Jr.*
Charles E. Mack, Jr.
Director of Research

ABSTRACT

Scattering distributions have been measured for Ar incident on fresh epitaxial Ag films. For several incidence angles, energies of 1 and 2 eV were supplied by a shock tube driven nozzle beam. Scattered density profiles in the plane of incidence and 30° out-of-plane agree very well in magnitude and direction with calculations for corresponding cases using methods described by Oman. No arbitrary scaling of density levels was employed. The scattering patterns are essentially unchanged for several hours at 5×10^{-7} torr. Peak signals are very high (> 10 times incident flux per steradian), and the small amount of excess flux near the surface normal suggests that most of the surface is atomically flat. Approximate measurements of reflected velocities agree well with predictions except between the specular and the normal, where measured velocities for the 1 eV case are quite low. Measurements by Romney and Anderson indicate good agreement with the same theory for direction and width of reflected beam as energy varies from 0.5 to 5 eV.

INTRODUCTION

The ability to predict momentum and energy exchange between a surface and a high energy [0(1 eV)] rarefied gas flow appears to be limited primarily because the interatomic potentials governing the interactions are not known. Numerical methods that include detailed physical states of the gas and the surface, and realistic geometric relationships are now available, and can be used to compute the dynamics of the interaction; however, the results of these calculations depend primarily on the choice of the potential (in effect, the atomic radius at a particular energy) used to describe the interaction. Before reliable predictions of aerodynamic forces, heat transfer, or surface chemistry can be made, better forms of the governing potentials must be found. We believe this can be done by combining complex three dimensional calculations with carefully performed scattering experiments using well-defined surfaces. Quantitative measurements of as many local properties of the scattered distributions as possible, using several related systems (e.g., the family of inert gases scattered by Ag) over a broad energy range, should provide the necessary information when combined with theory to determine the governing potentials. Our experimental methods give three dimensional quantitative measurements of the scattered density and mean velocity distributions as a function of the incident beam conditions. These

data are compared to the results of a very complex three dimensional numerical model developed by Oman and coworkers.^{1,2}

Theoretical Methods

Many theoretical models of gas surface interaction have appeared in the literature in recent years (cf., the review by Hurlbut³). These models may be loosely categorized as hard cube and soft cube theory, lattice theory, parameterization of distribution functions, and numerical experiment. All of these models assume particular forms for the interaction potentials that are based on extrapolation of concepts related to gas-gas interactions; in the epithermal energy range, even the potentials of the gas-gas problem are not well established. The degree to which any of the above models represent the real interactions can only be determined from good experiments in the appropriate energy range with particular emphasis placed on surface characterization (crystallography and atomic cleanliness).

The theory we developed over the past several years is described in Refs. 1 and 2. It is perhaps best understood as a numerical experiment designed to reproduce, as faithfully as possible, the geometry of the encounter. The major drawback of the method as it stands is that it requires a fairly large computational effort to get statistically reliable flux distributions (about 5 minutes on an IBM 360-75 yields 100 trajectories on the exit hemisphere, a number which will give, after interpolation,

fluctuations in spatial distributions usually less than 20% if the peak flux is as large as 10 units of incident flux per steradian). The method depends on numerical integration of the classical equations of motion for a series of gas atoms impinging on a system of harmonic oscillators. The oscillators are usually assumed to be independent of each other, and linked to the gas particle by an assumed pairwise potential. To date we have used only the Lennard-Jones 6-12 potential, but evidence discussed in this paper indicates that better choices can now be considered as a result of the comparison between complex theory and epithermal experiment. Several features, such as thermal motion in the lattice, contaminants on the surface, variations in lattice structure, coupling between lattice oscillators, and internal degrees of freedom for a diatomic gas particle have been incorporated, and can be included whenever desired.

Thermal and Structural Scattering

The theory predicts average momentum and energy states for the reflected atoms, and spatial distributions of various moments (e.g., density, flux, mean velocity, etc.) of the local velocity distribution. In this report we present several calculations of the local density ratio (i.e., the fraction of the exit density field that passes through a given local unit solid angle), the property we measured in the present experiments. From the laboratory and theoretical data we present here, it is not possible to

determine the trends of the distribution with changes in incident energy or angle, but the trends noted in our previous calculations and in the data of other workers are consistent with the present, more detailed, cases. For placing the present cases in proper perspective, it is useful to review briefly the concept of two regimes, denoted by thermal and structural scattering.²

The dominant effect in thermal scattering is the thermal motion of the surface atoms. In this regime, the scattered distribution becomes narrower (with a correspondingly higher peak magnitude) as the incident energy is increased. The change in tangential momentum in the reflection is usually small, because the potential field of the surface is quite smooth at the penetration level reached by the (relatively) low energy gas atom. The direction of the peak also shifts toward the tangent in thermal scattering as the incident energy is increased. Structural scattering, on the other hand, is characterized by the dominance of the individual atomic sites as scattering centers, thereby giving a much more broadly scattered distribution and a reversal of the above trends with energy. Structural scattering occurs at much higher incident energy for a given system of species and incidence angle. The change in tangential momentum is often quite large, and out-of-plane scattering is quite pronounced.

The transition from thermal to structural scattering does not appear to be sudden. Its exact features are still masked by statistical fluctuations in the theoretical distributions, and by a generally insufficient quantity of both kinds of data. It appears that the transition shows up at different energies for different features of the distribution; e.g., the turn-around in peak direction occurs at a lower energy than the turn-around in peak magnitude or in $\frac{1}{2}$ -magnitude width. Thus, the transition is best described as a region, not a discrete energy level for a given system. The transition appears to depend most strongly on the size of the colliding atoms relative to the spaces between atoms in the lattice; thus a different lattice structure may greatly affect the character and position of the transition range, even for the same gas and surface species. The present work, limited to the tightly-packed (111) plane of silver surfaces, shows very different behavior from that of a more loosely packed surface, such as the (100) bcc tungsten surface.

Previous Experiments

Five previously reported gas-surface interaction experiments in the epithermal energy range included attempts to ensure clean surfaces.⁴⁻⁸ Alcalay and Knuth⁴ reported qualitative in-plane density scattering distributions from epitaxially deposited Ag films for 1 eV and 1.2 eV argon beams. No clear trends were

established, but there was evidence that all of their distributions exhibited unexpected multiple lobes. One of the lobes would typically lie in the vicinity of the specular direction. The most surprising result was the presence of strong back-scattered peaks in all of their data. Subsequent density distribution data (Ref. 5) obtained in the same laboratory showed broadly scattered fields with no clear peaks. These data are not consistent with our present data, or with that reported by Romney and Anderson.⁷

The operational procedure described in Ref. 4 suggests that Alcalay and Knuth allowed their surfaces to cool below the temperatures recommended for epitaxial formation during the time of deposition. It is also likely that the 300°K temperature maintained during the series of experiments described in Ref. 5 resulted in much higher surface contamination levels than those present in the other investigations, because residence times of weakly bound adsorbates are exponential functions of surface temperature. We therefore conclude that the data of Refs. 4 and 5 are not representative of scattering from clean, epitaxial surfaces. However, the fact that most investigators find behavior that is suggestive of more ideal surfaces should not be construed as proof that any of the subject surfaces are clean or ideal.

O'Keefe⁶ scattered argon beams (.25-2.0 eV) from bcc (100) tungsten single crystals. The test surface was carefully characterized by electron microscopy and reflected high energy electron diffraction before being placed in the test chamber. Surfaces were cleaned by electron bombardment heating, and the chamber was maintained at 10^{-10} torr. During the experiment a measure of the amount of gas coverage (adsorption) on the surface was obtained by using retarding-field diode measurements of the surface work function. This work is especially important because absolute values of the scattered density distributions were reported as a function of incident beam energy and attack angle. For a variety of surface temperatures the distributions could be described as a single, strongly directed, very narrow lobe between the specular and the tangent for all energies investigated. In spite of the great care taken in these experiments, attempts to compare them with our theory have been questionable, largely because the test surface was hydrogen-saturated for all of the distributions presented, and we do not know enough about the H-W bond configuration to produce an unequivocal calculation.

Romney and Anderson⁷ scattered argon beams (.05-5.0 eV) from epitaxially deposited Ag films. The surfaces were characterized by X-ray and electron diffraction methods and found to be a strongly oriented fcc (111) surface. The presence of some unknown contaminant on the surface was noted, but there is no way of knowing whether it was present during the experiment. Surface cleanliness was occasionally

checked during the experiments by observing helium beam scattering patterns as suggested by Saltsburg and Smith.⁹ The scattered density distributions obtained by Romney and Anderson can be described by a single directed lobular peak over the entire energy range. The distributions were plotted in arbitrary units and indicated excellent agreement with the thermal energy data of Saltsburg and Smith.⁹ The variations with incident energy of the peak direction and the half-width of the distribution agreed quite favorably with the theoretical predictions of Oman.²

In a recent work Miller and Subbarao⁸ have measured directions of peak signal and angular width at $\frac{1}{2}$ -amplitude for neon and argon beams on epitaxial silver (111) films. Their incident energies range 0.06 to 2.5 eV. They found evidence of a clear transition from thermal to structural scattering in both systems, and were able to offer some correlating relationships to relate the energies of transition to incident angle in each case. It appears that their values for transition energy, particularly in the case of argon, are somewhat lower than that indicated by the behavior of the present results, although the clear trends they present appear to confirm the qualitative features of the expected behavior.

In this report, measurements of the absolute magnitude of the density field and mean velocity field resulting from the scattering of 1eV and 2 eV argon beams from freshly deposited epitaxial silver films are compared to predictions of the theory described in Refs. 1 and 2. Experiment and calculations are compared both in and out of the incident plane.

EXPERIMENTAL FACILITY

A shock tube terminated with a hypersonic nozzle was used as a source for obtaining epithermal energy in high intensity molecular beams of a wide variety of gases. Devices of this type have been described by Skinner,¹⁰ Jones,¹¹ and in several of our contract reports.¹²

The short test times of these facilities present some advantages; they offer a very high signal/noise ratio due to low background, high intensity, and the pulse nature of the signal. They do not present large vacuum pumping requirements or the associated back pressure effects on beam formation, and they offer the opportunity to control precisely the exposure of a surface to gas between its preparation and its investigation. Their principal disadvantage is that data acquisition rate is low.

A planform schematic of the Grumman molecular beam facility is shown in Fig. 1. The shock tube, operated in the reflected mode, provides a high temperature test gas for several milliseconds. Hypersonic expansion in a conical nozzle converts most of the stagnation energy into translational energy. The core of the expanded flow is collimated using two, and sometimes three, conical skimmers, while the remainder of the flow field is rejected into a large outer vacuum chamber. After collimation the beam passes into the test chamber where it strikes the target

surface. The reflected density distribution is measured using electron bombardment detectors that are mounted on circular hoops centered at the target location. Measurements of the time of flight between an appropriate reference location and the detectors are often used to obtain mean values of the incident and reflected beam velocities, although this is only possible under certain conditions.

The angle of attack between the target normal and the incident beam, as well as the position coordinates of the detectors can be varied to an accuracy of a few tenths of a degree from outside the test chamber, without loss of vacuum. External control of the detectors is limited to one degree of freedom, that is, the detectors are fixed on the hoops at particular values of ψ , the angle relative to the plane of incidence (see apparatus-oriented coordinates in Fig. 2). The hoops can be rotated to new positions (i.e., values of θ) before each shock tube run; the out-of-plane detectors describe arcs in planes that are parallel to the plane of incidence.

Targets

In the present series of experiments we employed the epitaxial deposition technique first used in molecular beam experiments by Saltsburg and Smith.⁹ This technique can be very useful in establishing a common standard between laboratories (cf., this report,

Saltsburg and Smith,⁹ and Romney and Anderson⁷), as well as in furnishing experimental surfaces that are strongly oriented fcc (111). Moreover, the surfaces appear to be clean and smooth to a very high degree on an atomic size scale. We deposited silver vapor from an electrically heated crucible onto a cleaved Muscovite mica substrate that was maintained at $555 \pm 10^\circ\text{K}$. The beam experiment can be initiated during deposition, or at any desired interval thereafter. Scattering patterns obtained with the Ag source active were the same as those obtained after cessation of the deposition for up to 24 hours in moderate vacuum of 10^{-7} torr. Most of our data were taken with the source inactive.

The target heater and vaporization source used in the deposition are not shown in Fig. 1. The target heater is simply a copper block heated by internal tungsten filaments. Surface temperatures are measured by using a chromel alumel thermocouple attached to the center of the block. The vaporization source was fabricated by wrapping and cementing (alumina cement) a .01" diameter tungsten filament about an alumina crucible. The evaporation source temperature was measured by monitoring the power input to the filaments after calibration against an optical pyrometer.

Detectors

The detectors used in our scattering experiments are specially constructed electron bombardment ionization gauges (Fig. 3). Our

design is a modified version of the through-flow type developed by Hagen and Henkes.¹³ A collimated ribbon of electrons perpendicular to the direction of flow produces an ion current that is proportional to the instantaneous local number density of the neutral molecules. We have determined the nominal sensitivity of several of these gauges in chopped effusive beams to be 10^{-12} microamps of ion current for $1 \text{ argon atom/cm}^3$, with 1 ma of emission current.

The neutral beam passes through the detector with no important attenuation because the flow is extremely rarefied, and only about one in 10^4 neutrals are ionized. This feature permits measurement of velocities between tandem detectors, and has been used in our more recent work to measure the incident beam properties during each run.

Detector Signal Processing

The output signal (ion collector current) of a detector is in the form of a pulse, the height of which is the local density during the test. Figure 4 shows typical signals for an incident beam (4a) and for the same beam after reflection from a surface (4b). In addition to the pulse height, it is often possible to extract a great deal of information about velocity distributions from the pulse shape. In principle this is simple, as a perfectly instantaneous start with a finite flight time results in a downstream

signal that is the integral of the flight time (inverse velocity) distribution. By electronic differentiation one can recover the function dn/dt , which is related to the distribution function expressed in terms of the axial velocity component, u , by the expression

$$F(u) = \frac{t^2}{L} \frac{dn}{dt} \quad (1)$$

where L = reference length, t = time measured from reference location, and n = number density $[\int_{L/t}^{\infty} F(u) du]$.

In practice there are some major difficulties in these measurements. The pulse is not a perfect step, the spread in arrival time of the incident beam limits the resolution of the reflected velocity measurements, and differentiating the traces greatly reduces the signal/noise ratio. By far the biggest problem, however, arises from the small amount of fluid that is processed by unsteady waves at the beginning of the nozzle flow period. In the unsteady process increased stagnation enthalpy is produced, resulting in flow velocities that are significantly larger than the mean steady flow value. The time-of-flight distributions therefore show a high velocity wing, as can be seen in the lower traces of Figs. 4a and 4b. In most cases the starting portions are well separated from the distributions for the established flow, so we have used them to estimate time-of-flight velocity when such is the case.

Although they are not very accurate, we believe that these measurements are meaningful, because velocity measurements in unskimmed flows downstream of nozzles made in our facility agree very well with calculated values for an ideal adiabatic expansion, and because measurements reported by Hagena,¹⁴ using pulsed molecular beams indicate that the mean velocity measured at the peak of the time-of-flight distribution is identical at the start of the pulse and at some later time.

RESULTS AND DISCUSSION

Absolute magnitudes of the density and velocity distributions for 1 and 2 eV argon beams scattered from epitaxially deposited Ag films are compared with predicted distributions obtained from Oman's theoretical model of the interaction. The coordinate systems used to define the positions of measurement are shown in Fig. 2. The theoretical calculations were performed using surface-oriented coordinates, but the resulting density field was computed in apparatus-oriented coordinates (right side of Fig. 2) for purposes of comparison with the laboratory data. The density data are presented as local values of ρ (the number density) divided by ρ_i , an equivalent measure of the incident beam. The ratio ρ/ρ_i represents the flux ratio (the fraction of the incident flux that emerges in a particular unit solid angle) amplified by the ratio of incident to local reflected velocity. The ρ/ρ_i ratio was obtained by dividing the measured reflected (density) signal per steradian of detector by the signal from an identical gauge that intercepts the entire incident beam. The velocity data are normalized in a similar manner. Averages of the incident beam properties obtained from repeated calibration runs were used in the normalizations in most of the data presented, although recently direct measurements have been used.

Density Distributions

Scattered density fields are shown in Figs. 5-8 for the plane of incidence and, in most cases, for 30° out of plane. Out of plane data are necessary to give a complete picture of the scattering process. From continuity considerations, one can see the integral of the flux ratio over the entire exit hemisphere must be equal to 2π . The out of plane data presently available are not sufficient to enable this type of calculation. We do, however, measure absolute values of the density fields, so that we can use the relative agreement between theory and experiment as a measure of species conservation, because material balance is implicit in the theory.

In Figs. 5, 6, and 7, the scattered density distributions are shown for a nominal 1 eV argon beam incident at 40° , 50° , and 60° with respect to the target normal. The plots show the fraction of the incident density per steradian as a function of the reflected in-plane angle θ . The theoretical distributions in Fig. 6 are the same data previously reported by Oman,² except that now the density is shown instead of the flux for that case. The data of Figs. 5 and 7 were calculated especially for this work, and the parameters used to describe the interatomic potentials in the theoretical model were selected² on the basis of a comparison with the 300°K neon/silver data of Saltsburg and Smith.⁹ Quantitative agreement between theory and experiment is

quite good, except in the vicinity of the target normal, where the experimental data for all test conditions consistently show an excessive density. As the incidence angle is increased the experimental distributions sharpen relative to the theoretical predictions, and the peak location deviates slightly toward the tangent from the predicted value. We suspect these departures from theory are partly a result of defects in the experimental surface; these defects become more apparent as the angle of incidence increases. The backscattered densities, in the vicinity of the normal, are about 1/2 to 1/4 of the magnitude that would be present if the reflection of the entire beam were diffusely distributed, but these magnitudes are roughly consistent with the fact that most of the experimental data near the peak are lower than the theoretical predictions.

The high directivity of the reflected distributions is apparent. About 15 times the incident flow would be necessary to fill one steradian at the peak levels of signal. However, the Ag (111) is a very tightly packed lattice. For a more open surface, such as a bcc (111), we would not anticipate such a strongly directed scattering pattern (cf., Ref. 6).

The data presented here have been replicated many times on several freshly deposited Ag surfaces. These data were obtained with a signal/noise ratio of 5 and greater. Errors in measurement

of the raw reflected-beam data were quite small compared to the uncertainty in the incident-beam density used in the normalizations for fixed incident beam conditions. Several different detectors were rotated into a particular set of reflected coordinates and the repeated density measurements agreed to within a few percent. Incident beam calibration indicated a $\pm 10\%$ variation about the average incident density used in the normalization. We estimate the over-all uncertainty at about $\pm 15\%$.

In Fig. 5 several different data symbols are used to indicate the use of different detectors in recording the data. By continuously monitoring signals with different detectors at fixed reflected coordinates, we were able to determine the surface condition relative to the original surface condition when the Ag source was active. We found that after the surface was exposed to the beam pulse approximately 6 to 8 times, the surface degraded in a discontinuous fashion; that is, the signal at a particular coordinate differed significantly from that obtained on the previous run. When we continued to survey the scattered field, new distributions were obtained. The new distributions were difficult to complete because after the transition there was a continuous slow variation of the signal at each measurement point from run to run.

Scattered density fields in plane and 30° out of plane are shown in Fig. 8 for a 2 eV argon beam incident at 50° with

respect to the target normal. The distributions obtained from a freshly deposited surface are indicated by open symbols, and the distributions from the same surface after it had changed character are indicated by filled symbols. For the fresh surface condition, we had a great deal of trouble obtaining reproducible peak magnitudes using the 2 eV beam. Peak magnitudes obtained using several different surfaces ranged from 15 to 21 per steradian. A large enough statistical sample is not available at this time (5 surfaces have been tested) to allow a meaningful average of the data and, therefore, we simply show the value that most frequently occurred. The measurement errors previously discussed for the 1 eV data should also be applied to these data.

The locations of the experimental peak magnitudes in the plane of incidence for both fresh and altered surfaces are in fair agreement with predictions at both 1 and 2 eV, and these measurements were replicated for all surfaces tested. The relatively poor agreement of the out of plane measurements for the 2 eV cases is consistent with the increased directivity observed in the corresponding in-plane data. Comparing the 1/2 widths of the experimental distribution at 1/2 maximum amplitude with theory for the 1 eV and 2 eV beams incident at 50° indicates that the difference in dispersion between theoretical and experimental distributions is much larger in the 2 eV case. A similar conclusion can be drawn by inspecting the qualitative distributions obtained in

Ref. 7 for 1 eV and 2.56 eV argon beams scattered from epitaxially deposited Ag films.

Exit Velocity

Velocity measurements using the time of flight technique and the differentiated density records were described in an earlier section. Some typical velocity data for the 2 eV incident beam are shown in Fig. 5. In Fig. 9 the in-plane mean velocity distribution is shown for the 2 eV argon, 50° incidence case. The plot shows the measured velocity, expressed as a fraction of the incident velocity, as a function of the reflected detector angle θ , and compared to the theoretical predictions.

The time of arrival at the target is calculated by using an average value of the beam velocity that was obtained in previous calibrations for the particular source conditions employed in the experiment. During the calibration, small variations in shock speed caused deviations from the average of velocity by as much as $\pm 10\%$. An additional error of $\pm 5\%$ was always present because of inaccuracies in reading the scope trace. For the worst case, the time of arrival at the target could be in error by approximately $\pm 12\%$. This uncertainty in time can represent a 20% error in the measurement of the reflected beam velocities when V/V_i is approximately unity because of the short reflected

beam path lengths (~ 18 cm). The measurements shown may be substantially better than the above implies because an E-put counter was used to measure the shock speed in the shock tube, and we could correct for small changes in shock tube conditions. In future experiments the incident beam signal will be recorded on every test run and the over-all accuracy of the measurements will be considerably improved.

Comparison with Previous Experiments

Experimental data reported by Romney and Anderson⁷ for scattering of argon beams in the energy range .05 eV to 5 eV from epitaxially deposited Ag films demonstrate qualitative agreement with our data and with that of Ref. 9. Romney's data also indicate that the trends in peak magnitude direction and in the half-width at half-maximum amplitude of the scattered density distributions based on Oman's model² are qualitatively correct. In Fig. 10, Romney's data for measured peak magnitude direction as a function of incident beam energy, with incidence angle fixed at 50° , are shown. Our data, Saltsburg and Smith's, our theoretical predictions, and predictions obtained from the hard cube model of Logan, Keck, and Stickney¹¹ are also shown. The discrepancy between the latter theory and experiment at the higher beam energies is to be expected because the assumptions made in their model are valid

only at low incident energy. In particular, we believe that the assumption of tangential momentum conservation does not apply when the incident gas atom becomes energetic enough (collision cross section becomes small compared to the nearest-neighbor spacing in the lattice) to penetrate into the lattice potential field. We believe it is this size dependence on energy (structural scattering) that is responsible for the peak direction reversal shown in Fig. 11.

We did not observe experimentally the change in amplitude trend in our 1 eV and 2 eV data, and Romney and Anderson⁷ have not observed it up to energies of 5 eV; although their two dimensional configuration might delay the apparent magnitude reversal a little. Since the trends depend on the size of the incident gas atom for fixed surface conditions, the turn-around energy for a neon beam should be much lower than that for an argon beam. We have some preliminary experiments with neon that indicate such is the case, but the expected behavior is shown clearly in the results of Miller and Subbarao.⁸ The main feature of our neon data is that the distributions are consistently more sharply directed (amplitude about twice as large) than predicted by calculations.

Surface Characterization

The 1 eV, 50° incidence scattering data for argon were used to define acceptable surfaces for all other experiments. Immediately after a surface was deposited, we measured the peak magnitude of the reflected signal for the above test conditions before proceeding with the new experiment. Subsequent changes in surface condition were observed by repeatedly measuring the reflected data at particular coordinates with several different detectors.

Quantitative analysis of several test surfaces was performed by the staff of our Materials Research Laboratory after the specimens were removed from the test chamber. X-ray diffraction patterns and electron probe microanalysis measurements were made on contaminated surfaces (exposed to argon beam) and on freshly deposited surfaces as well as on the mica substrates and silver removed from the sides of the oven. The results of these studies are summarized below.

The X-ray diffractometer traces indicated that the deposited silver films have an fcc lattice structure that is almost completely oriented (> 95%) along the (111) planes. The presence of two impurity phases was also evident in these traces. Both impurities were indicated as bcc (211) surfaces. One of the impurities had a unit cell parameter of 4.601\AA , and it was suggested

that this might be the cubic compound Ag_4O_3 which has a reported¹⁶ lattice parameter of 4.55\AA . The other impurity could not be identified because its measured lattice parameter of 5.09\AA could not be associated with any of the reported oxides of silver. Silver oxides were sought because the electron probe fluorescence scan of all elements with atomic number ≥ 5 indicated the presence of only silver and oxygen. Both of the surface diagnostic methods showed significant increases in impurity content on those surfaces that had been exposed to argon beams.

Romney and Anderson⁷ also report that surface analyses conducted on test surfaces after their removal from the test chamber indicate the presence of impurities. These impurities showed a bcc structure and a lattice parameter of 5.52\AA . Since their 1 eV scattering data are in such excellent qualitative agreement with ours, one might speculate that none of these impurities were present during the experiments; that is, the surface contamination occurred after the surfaces were exposed to the laboratory environment. If this is the case, then the differences in oxide concentration cited above for our surfaces could be due to slow oxide formation at room temperature,¹⁷ since the beam-exposed target was aged in atmosphere significantly longer than the freshly deposited target. On the other hand, the changes in the magnitude of the scattered molecular beam signal observed in our experiments after

many beam exposures might be the result of surface degradation caused by repeated interaction between solid or gaseous shock tube contaminants and the target. Visual inspection of the test surfaces at 150 power after repeated beam exposure did not indicate any physical damage, but a faint outline of the beam impingement ellipse is visible with the naked eye under certain lighting conditions. Vapor-deposited surfaces obtained in our laboratory and elsewhere^{7,8} did not appear to be contaminated for very long time periods in moderate vacuums of 10^{-6} to 10^{-7} torr, even after deliberate exposure to a variety of reactive gases, as long as the surfaces are kept at about 560°K .

Saltsburg and Smith⁹ suggested that the most likely reason for the stability of their surfaces was the formation of a strongly bound contaminant layer during deposition. They postulated that slow adsorption of a more weakly bound layer during vacuum aging resulted in the observed surface degradation. The findings of our surface studies are not inconsistent with their mechanism, but neither do we have any evidence to support it. The question of surface contamination and its connection to beam exposure obviously needs further study.

CONCLUSIONS

The results we have obtained indicate that three dimensional numerical calculations of the scattered density fields resulting from the interaction of argon atoms with fcc (111) Ag films are in good quantitative agreement with several independent measurements. Specifically, the fraction of the incident flow that is scattered into a particular solid angle is found to be consistently close to theoretical predictions, of both in and out of the plane incidence. Furthermore, the data obtained by Romney and Anderson⁷ as well as data obtained in our work demonstrate that the predicted energy trend reversals in peak direction and distribution occur at about the expected value of incident energy.

The peak intensities of the reflected beams are much higher than those measured in the work of O'Keefe and French,⁶ the only previous case in which quantitative intensity measurements were made. We believe the difference is due primarily to the fact that the tungsten (100) surface used by O'Keefe and French is much less tightly packed than the silver (111) used here (the area per surface atom is 2.77 times greater for the tungsten surface, yet the surface nearest-neighbor distances are nearly equal; 3.16Å for tungsten versus 2.86Å for silver). In the structural scattering domain, this difference in apparent roughness [the tungsten (100) shows a large pit in the center of each cell]

should make a very large difference in the widths of the observed scattering pattern. It is possible that the thermal and structural scattering domains would merge in the case of such an "open" lattice, and the trend reversal might be much more difficult to detect.

A few tests using neon at different energies on Ag (111) have shown reflected peak directions about right, but magnitudes about twice as large as those predicted by the calculations in Ref. 2, which are not statistically reliable for these cases. The trends of these distributions with energy, however, do indicate that the transition from thermal to structural scattering does take place in the general vicinity of 0.3 eV, which is well within the predicted range. This behavior is particularly interesting in view of the fact that helium scattered from Ag (111) consistently produces very sharply scattered beams, while the corresponding theoretical distributions are very broad. We currently feel that the implicit connection in the Lennard-Jones 6-12 potential between the attractive binding energy, ϵ , and the strength of the repulsive force at a given short-range position (also proportional to ϵ) is misleading. At this time it appears that we should seek a family of potentials that would allow the short-range forces to remain strong (giving larger-looking atoms), while the attractive bond grows weaker as lighter noble gases are used.

ACKNOWLEDGMENTS

Among the many who aided in this work, we would like to thank especially Dr. Howard Saltsburg, who aided us in our initial efforts with epitaxial deposition in situ, and Drs. Michael Romney and James Anderson, who gave us early access to their data.

REFERENCES

1. R. A. Oman, A. Bogan, C. Weiser, and C. H. Li, AIAA J., 2, 10, 1722 (1964); see also R. A. Oman, AIAA J., 5, pp. 1280-7 (1967).
2. R. A. Oman, RGD 6, Vol. II, p. 1331-44. See also R. A. Oman, J. Chem. Phys., 48, 3919-29, 1968.
3. F. C. Hurlbut, Proc. Intern. 5th Symp. Rarefied Gas Dyn., C. L. Brundin, ed; Academic Press, 1967, Vol. I, pp. 1-34; such symposia hereinafter designated RGD 5, etc.
4. J. A. Alcalay and E. L. Knuth, RGD 5, Vol. I, pp. 253-68.
5. J. P. Callinan and E. L. Knuth, RGD 6, L. Trilling and H. Wachman, ed; Academic Press, 1969; Vol. II, pp. 1247-56, 1247 (1969).
6. D. R. O'Keefe and J. B. French, RGD 6, Vol. II, pp. 1279-98.
7. M. J. Romney and J. B. Anderson, J. Chem. Phys. (to be published, 1969); see also M. J. Romney, Ph.D. Thesis, Princeton U., 1969.
8. D. W. Miller and R. J. Subbarao, J. Chem. Phys., 51 (to be published, November 1969).
9. H. Saltsburg and J. N. Smith, Jr., J. Chem. Phys., 45, 2175 (1966).
10. G. T. Skinner and J. Moyzis, Phys. Fluids, 8, 452.
11. T. V. Jones, RGD 5, Vol. I, pp. 1393-1406.

12. R. A. Oman and V. S. Calia, "A Shock Tube Driven Molecular Beam for Gas-Surface Interaction Experiments," Grumman Research Department Report RE-223, August 1965.
13. O. Hagena and W. Henkes, Z. Naturforschg, 15a, 851 (1960).
14. K. Bier and O. Hagena, RGD 4, J. H. de Leeuw, ed; Academic Press, 1966, Vol. II, 260-78.
15. R. M. Logan, J. C. Keck, and R. E. Stickney, RGD 5, Vol. I, pp. 49-66.
16. J. Vlach and B. Stehlik, Collection Czech. Chem. Commun., 25, 676 (1960).
17. D. O. Hayward and B. M. W. Trapnell, Chemisorption (Butterworths Scientific Publications Ltd., London, 1964), 2nd ed., p. 73.

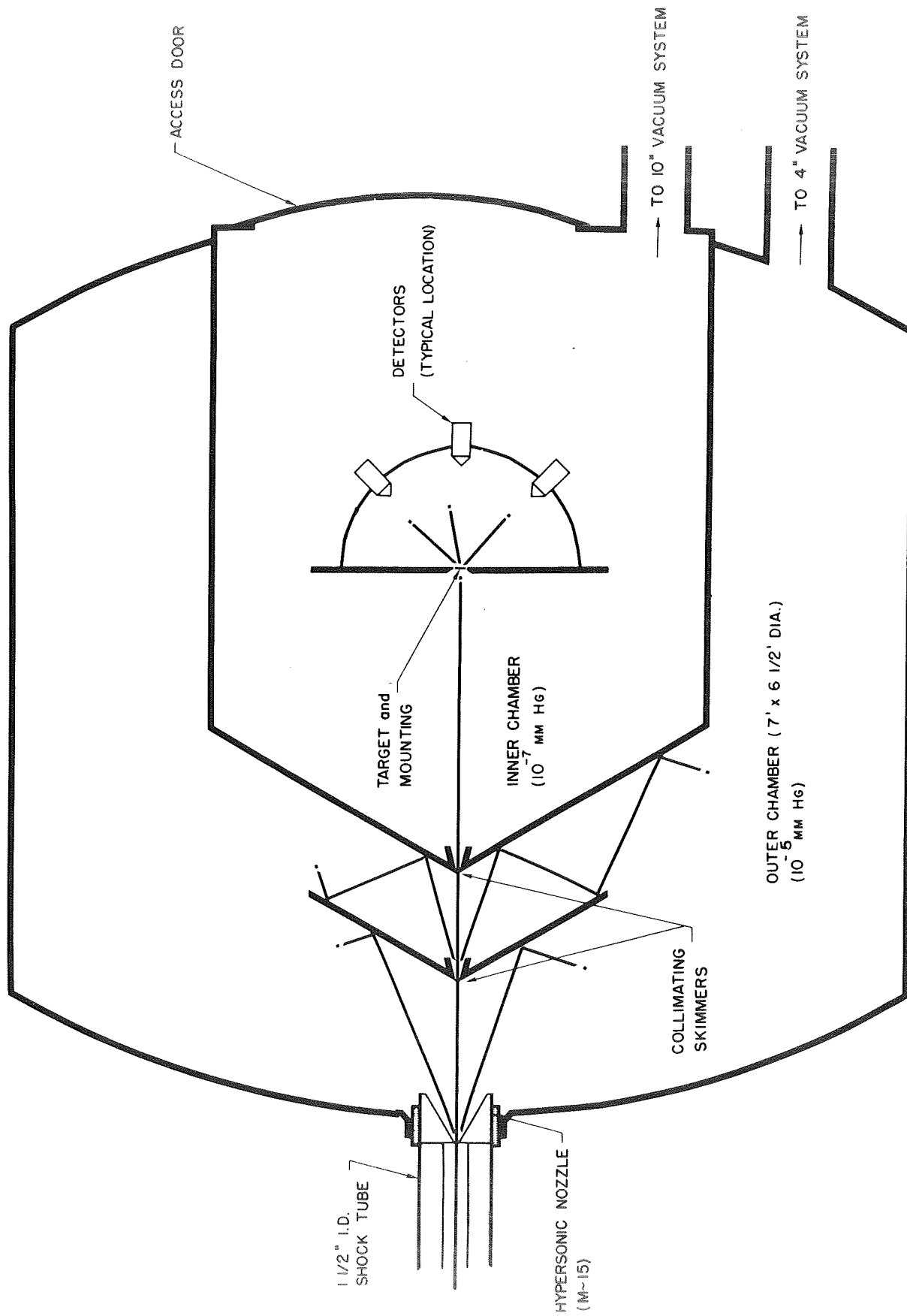


Fig. 1 Schematic Diagram of Molecular Beam Apparatus

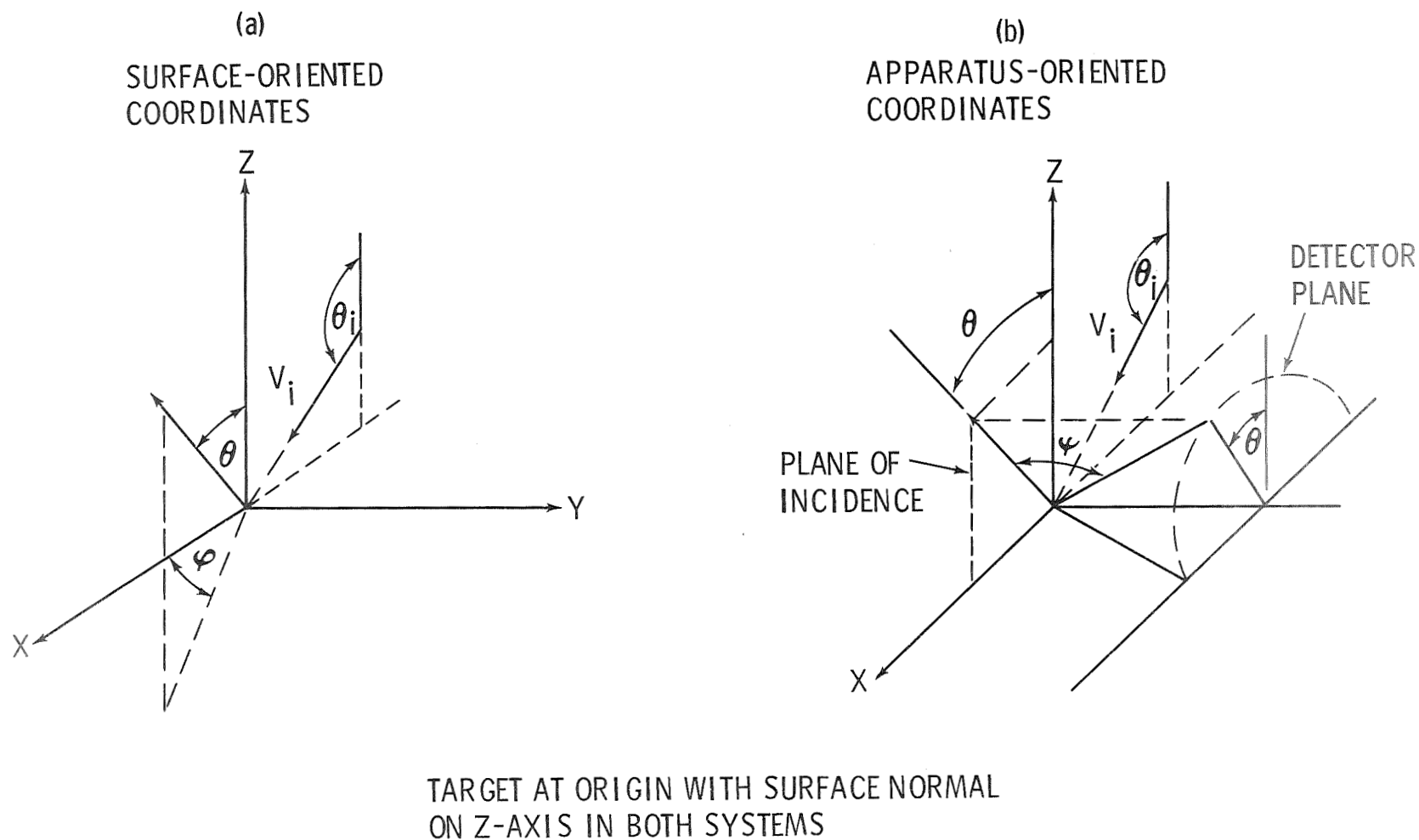


FIG. 2 COORDINATE SYSTEMS USED IN THEORETICAL MODEL (a), AND IN EXPERIMENTAL FACILITY (b)

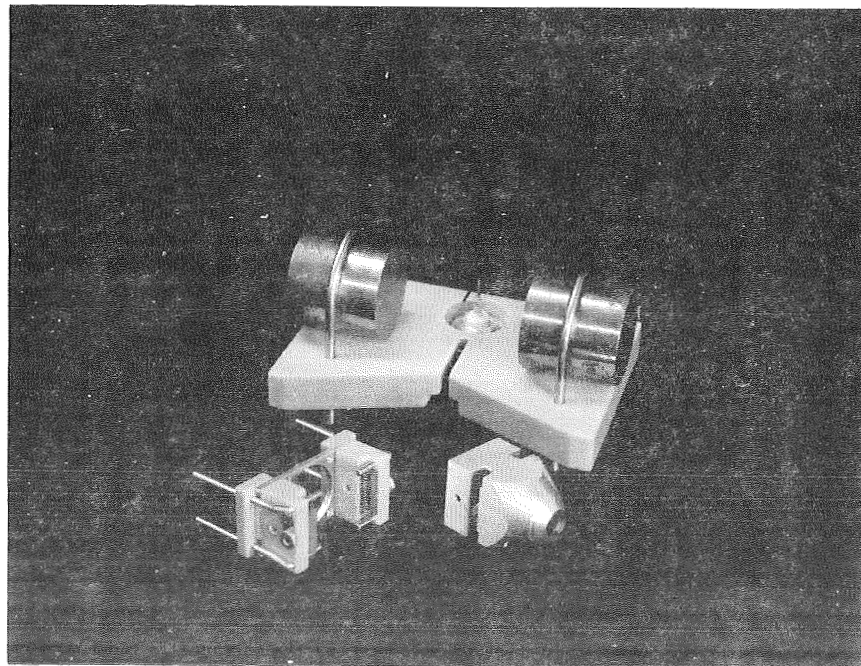
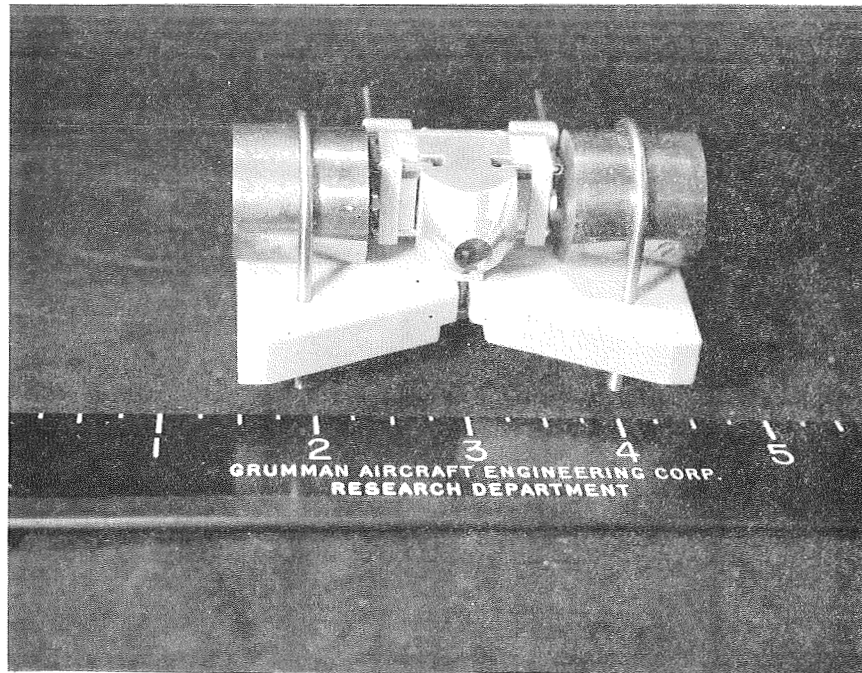
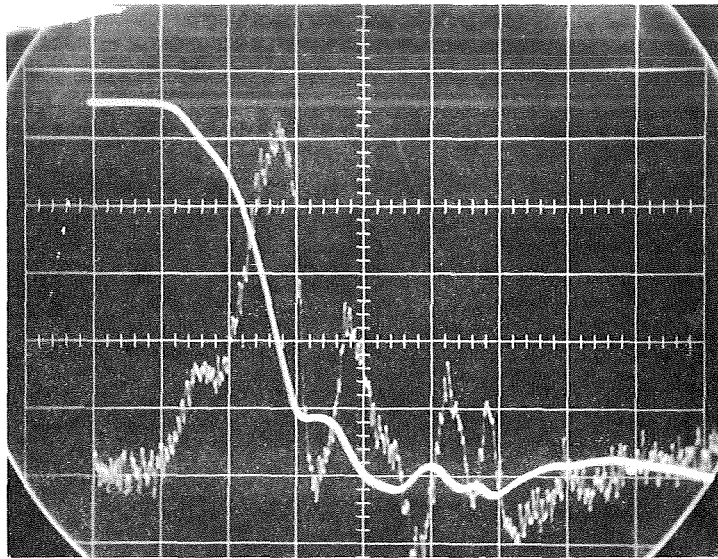


FIG. 3 PHOTOGRAPHS OF THE DETECTOR



100 μ S/CM

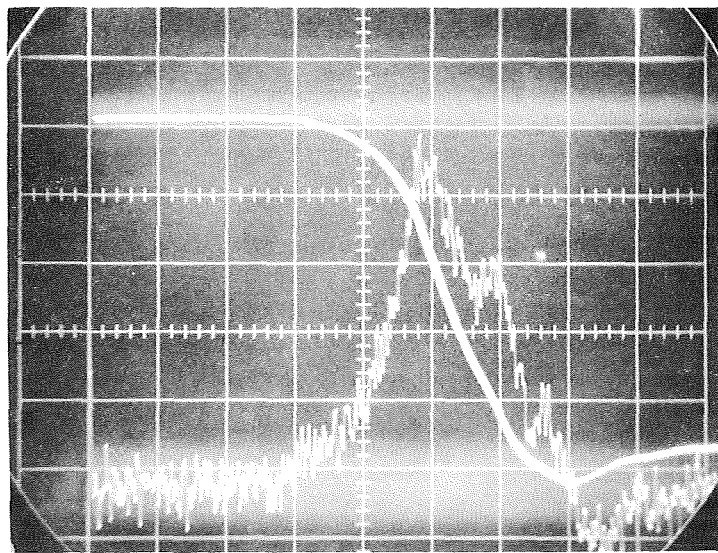
50 MV/CM



(A) INCIDENT BEAM



2.0 V/CM



100 μ S/CM

2.0 MV/CM



(B) REFLECTED BEAM
AT $\theta = 57^\circ$, $\psi = 0^\circ$



2.0 V/CM

UPPER TRACE: SIGNAL AMPLITUDE PROPORTIONAL TO INSTANTANEOUS LOCAL NUMBER DENSITY

LOWER TRACE: SIGNAL AMPLITUDE PROPORTIONAL TO dn/dt

FIG. 4 TYPICAL SIGNALS FROM DETECTOR FOR A 2eV ARGON BEAM

Ar/Ag (111) $E_i = 1.0$ eV

40° INCIDENCE

$T_{\text{wall}} \approx 560^\circ$ K

FILLED SYMBOLS, $\psi = 30^\circ$

OPEN SYMBOLS, $\psi = 0^\circ$

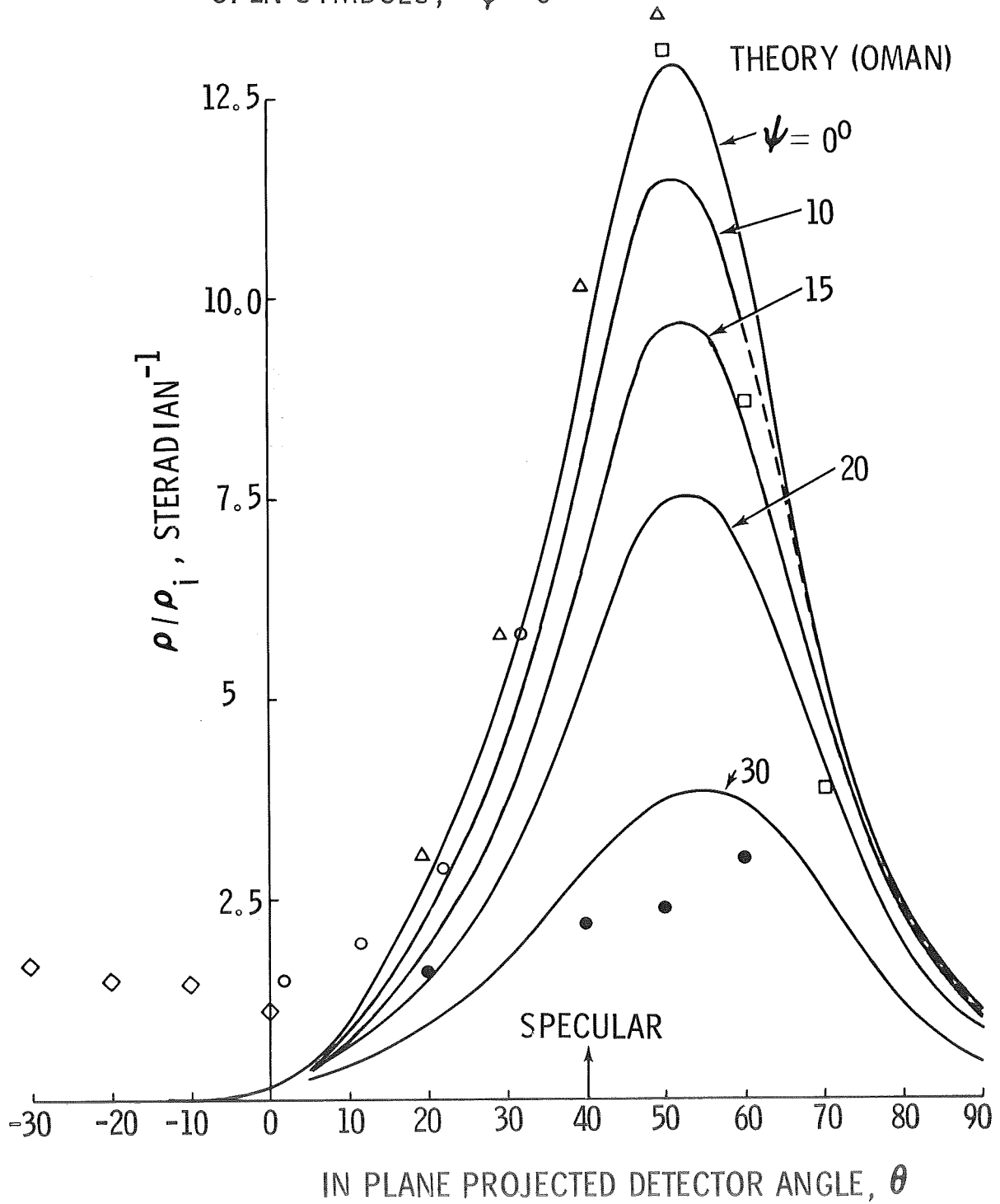


FIG. 5 COMPARISON OF LOCAL REFLECTED DENSITY RATIO FROM THEORY AND EXPERIMENT

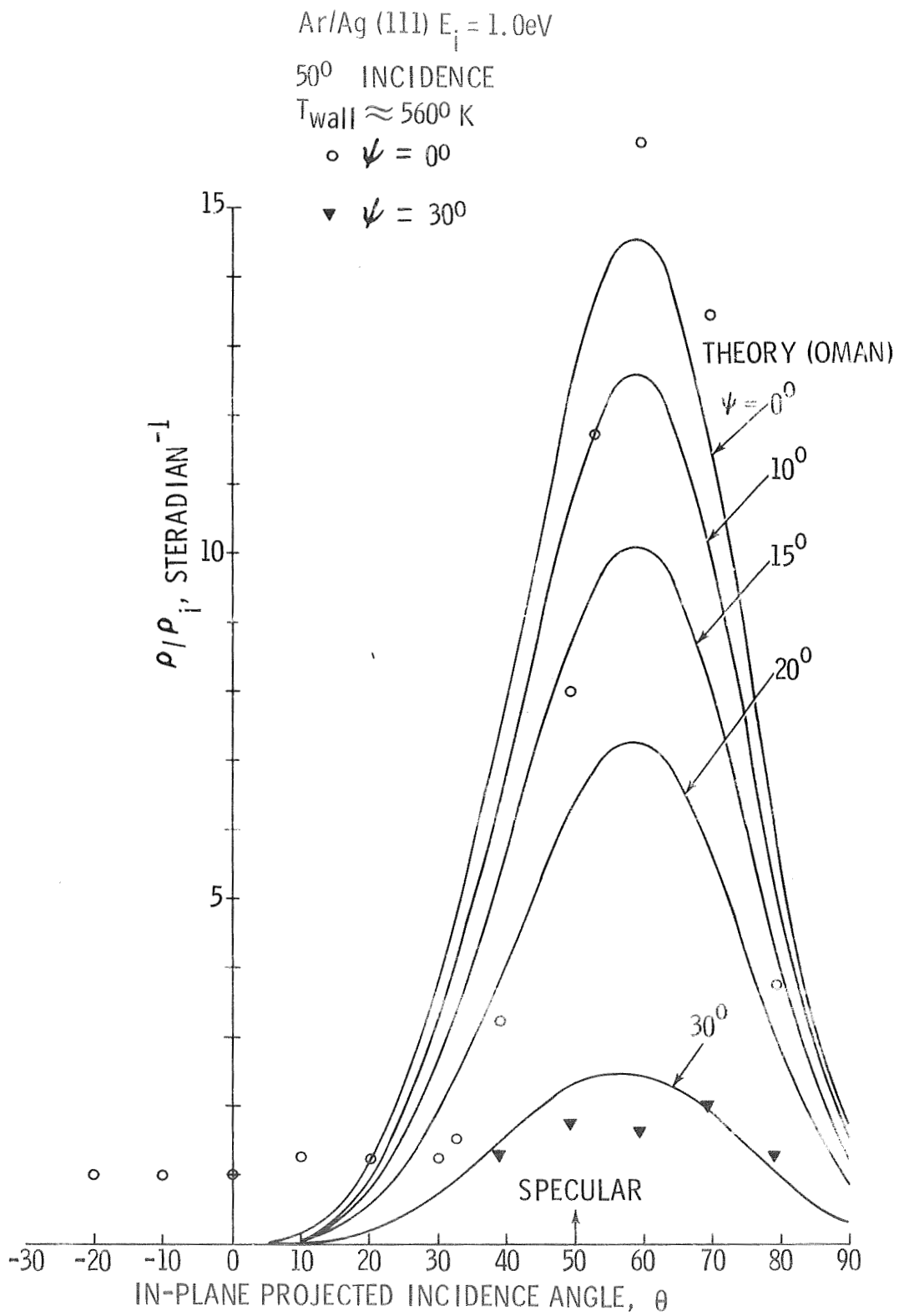


FIG. 6 COMPARISON OF LOCAL REFLECTED DENSITY RATIO FROM THEORY AND EXPERIMENT

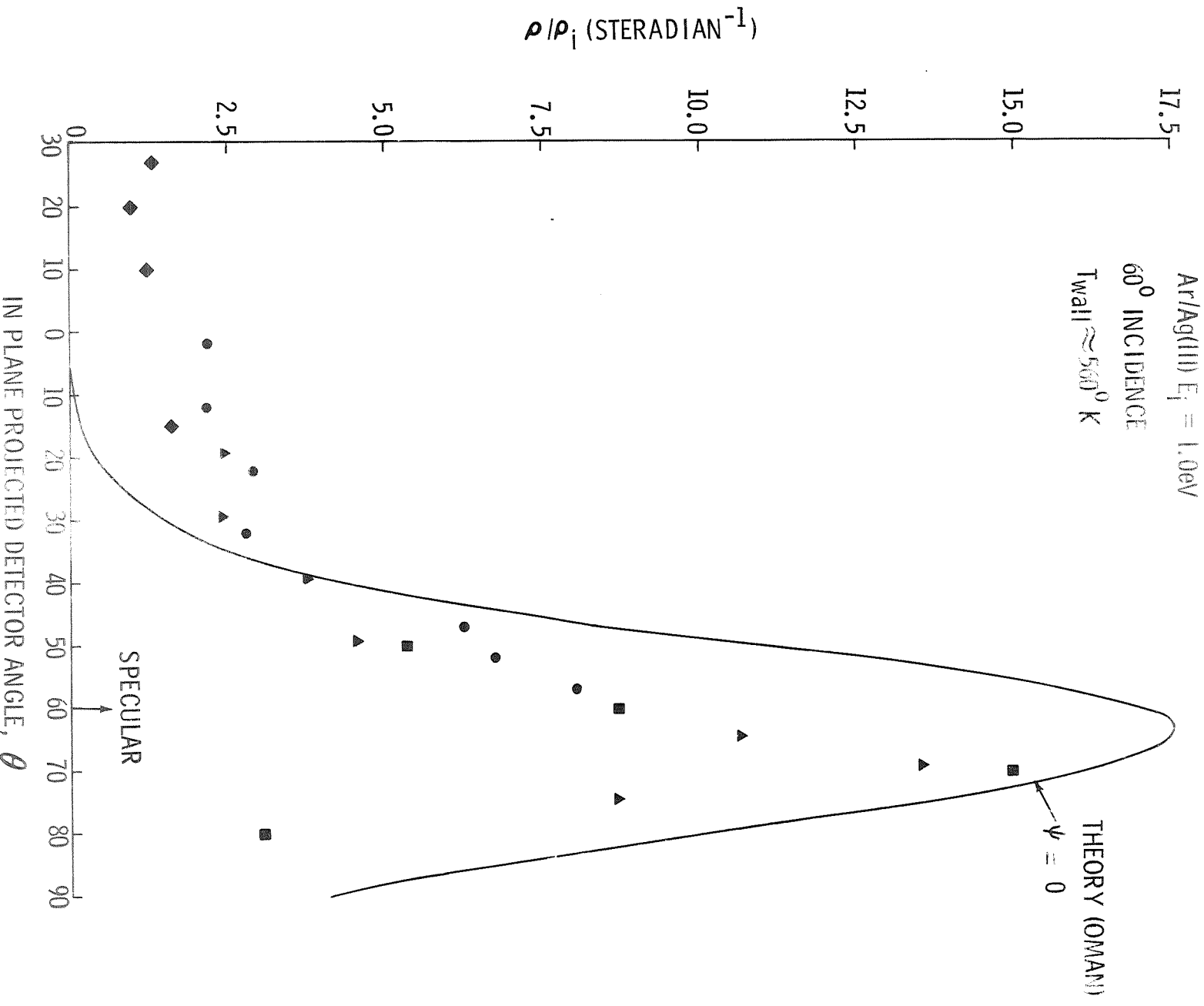


FIG. 7 COMPARISON OF LOCAL REFLECTED DENSITY RATIOS FROM THEORY AND EXPERIMENT IN THE PLANE OF INCIDENCE

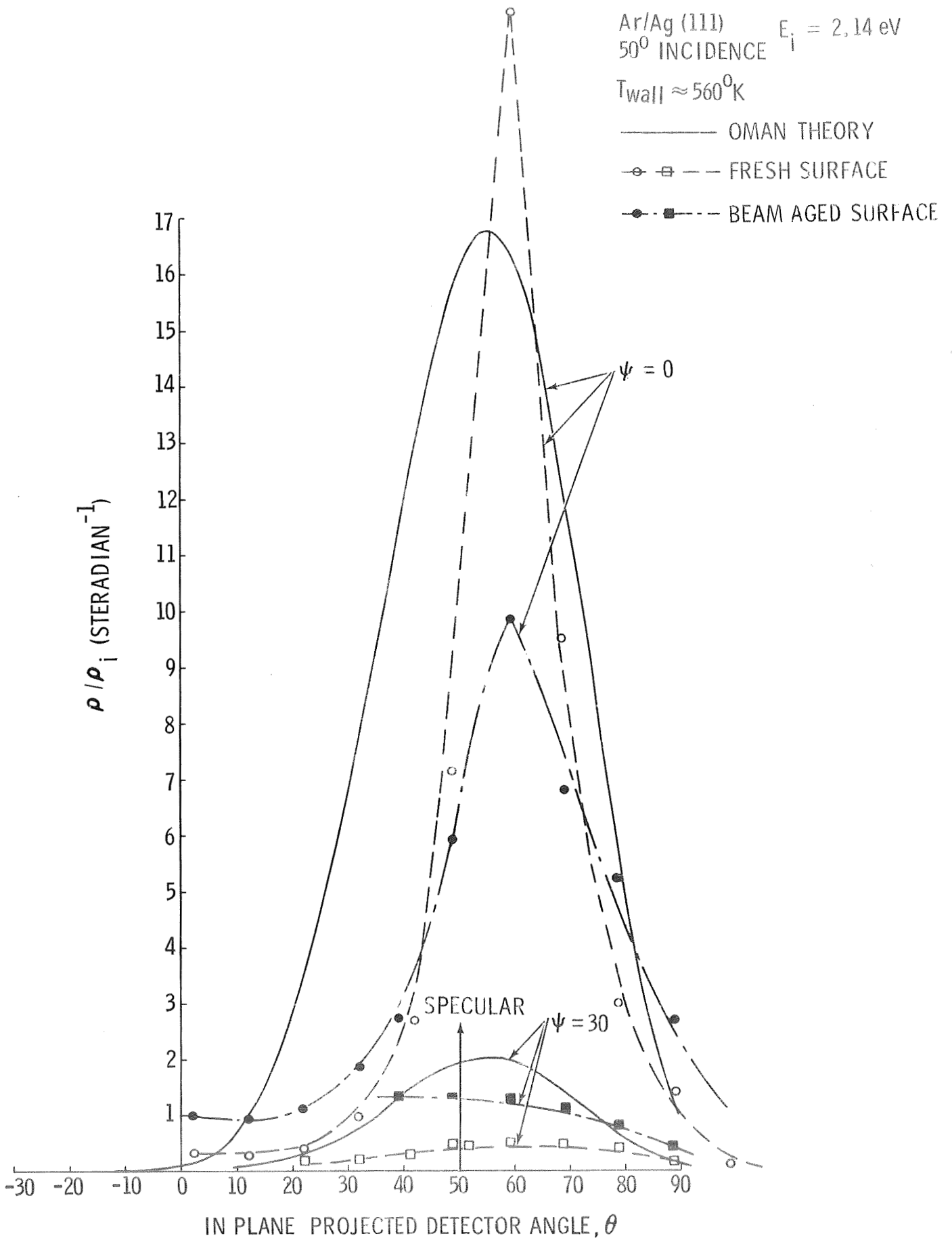


FIG. 8 COMPARISON OF LOCAL DENSITY RATIO FROM THEORY AND EXPERIMENT - EFFECTS OF AGING

Ar/Ag (111) $E_i = 2.14$ eV

50° INCIDENCE

$T_{\text{wall}} \approx 560^\circ\text{K}$

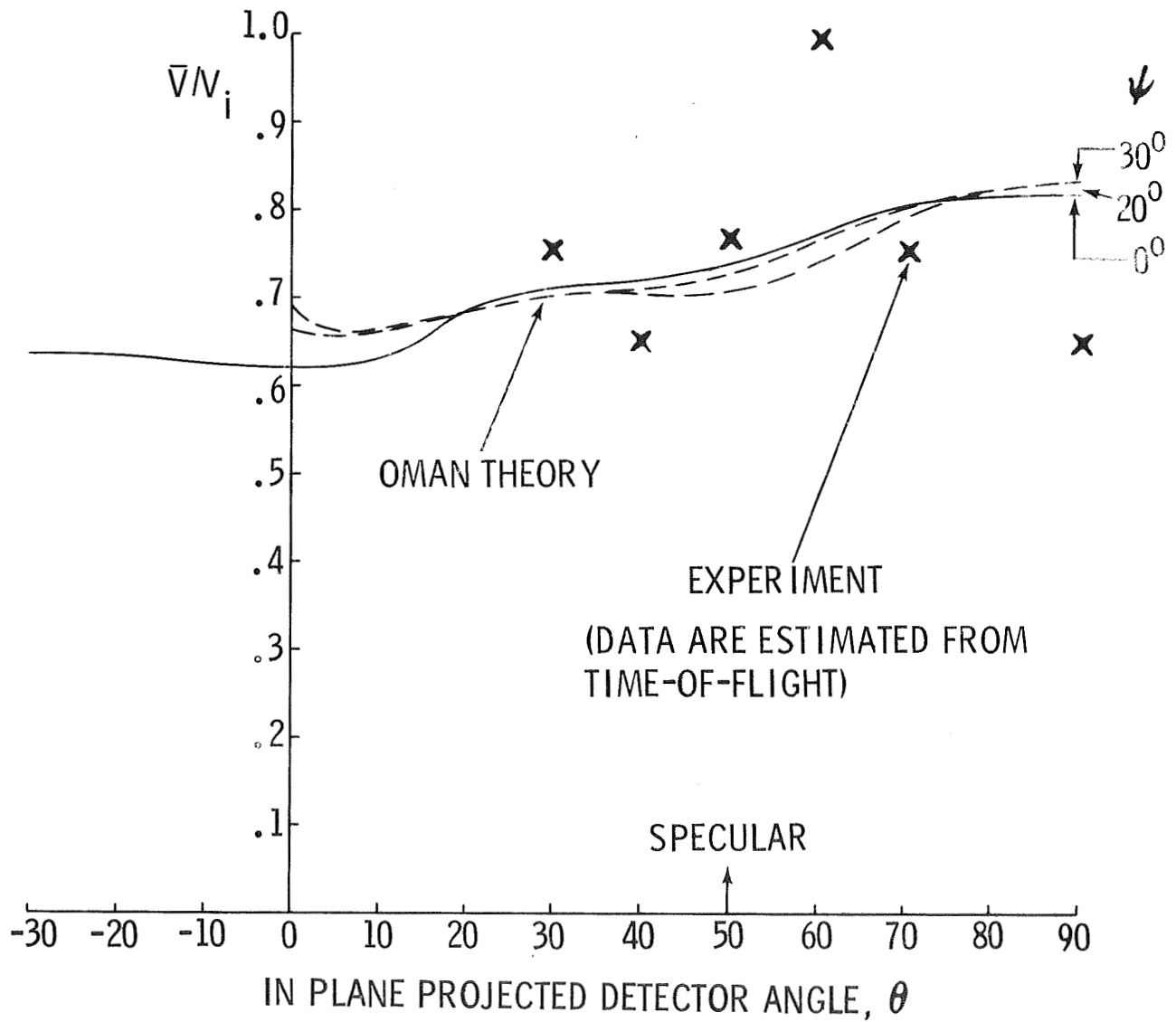


FIG. 9 COMPARISON OF LOCAL MEAN EXIT VELOCITY RATIO FROM THEORY AND EXPERIMENT

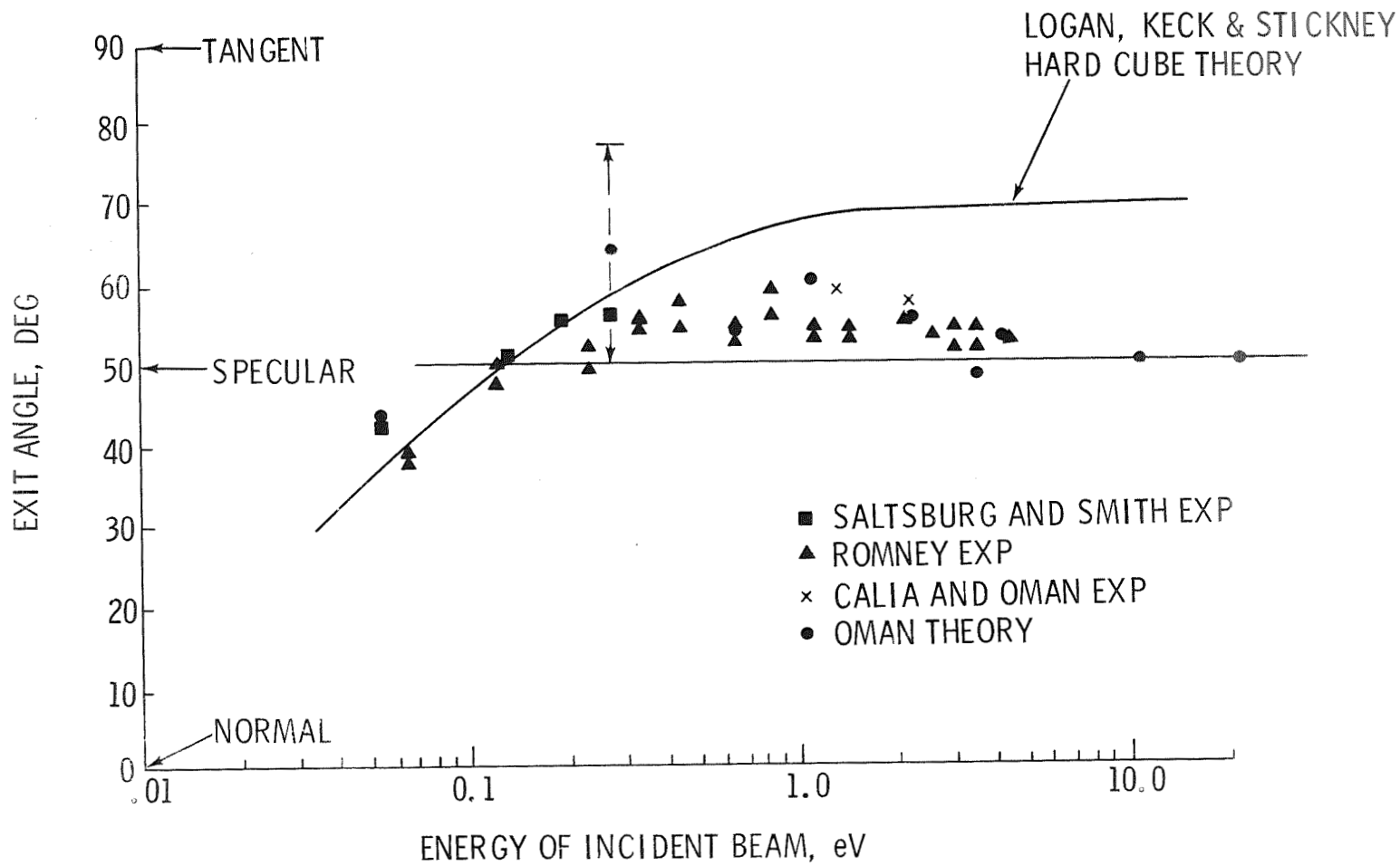


FIG. 10 SCATTERED PEAK DIRECTION AT 50° INCIDENCE ARGON/(111) SILVER



GRUMMAN AIRCRAFT ENGINEERING CORPORATION
BETHPAGE NEW YORK